Egyptian Journal of Radiology and Nuclear Medicine

RESEARCH

Open Access

Lung infections in HIV-infected children: imaging pattern recognition and its correlation with CD4 counts

Vishal Goel[1], Mahender K. Narula[2], Shahina Bano[3], Rama Anand[2], Vikas Chaudhary[2*], Varinder Singh[4] and Sonal Saxena[5]

Abstract

Context Children with human immunodeficiency virus (HIV) infection frequently present with opportunistic infections of the lung that may be associated with high mortality rate. There is no study, to the best of our knowledge, correlating specific radiographic patterns of chest infections with CD4 levels of immunity in HIV-infected children of Indian subcontinent (where prevalence of respiratory tuberculosis is very high).

Aims To study the radiological patterns of chest infections in HIV-infected children, and to correlate these radiological findings with CD4 cell count and final diagnosis.

Methods Forty-five HIV-infected children (1–18 years of age) with suspected chest infections were included in the study. The baseline and the most recent CD4 counts were recorded for each patient. Chest X-ray (CXR) was obtained in all the patients, and multi-detector computed tomography (MDCT) chest was done in 27 patients having clinical suspicion of infection with normal or equivocal findings on CXR. Chest radiographs and MDCT chest were analyzed for different radiological patterns of chest infections. Imaging findings were correlated with CD4 count range for disease spectrum. The final etiopathological diagnosis was achieved in combination with clinico-radiological findings, laboratory data, cytohistopathology and follow-up imaging.

Results Out of 45 children confirmed to be HIV-infected, 27 (60%) had bacterial infection, 14 (31.11%) had tuberculosis, and four (8.89%) had fungal infection.

Consolidation on CXR/CT strongly suggested bacterial etiology ($P < 0.05$). Mediastinal/hilar lymphadenopathy (with or without necrosis) strongly suggested tubercular etiology (P value < 0.05). Diffuse GGO/haziness on CXR/CT strongly suggested fungal etiology (P value < 0.05).

On correlation with CD4 count (cells/mm^3), the bacterial infections occurred at early stages of HIV infection when immune status was relatively preserved, and most of the patients with tubercular infection had moderate immunosuppression. On the other hand, all patients of fungal infection showed severe immunosuppression.

Conclusion A wide spectrum of pulmonary disease encountered in HIV-infected children warrants an integrated approach of image interpretation. Familiarity with the imaging patterns, combined with relevant clinical/laboratory details, may greatly help to improve the diagnostic confidence and to reach to a more meaningful differential diagnosis.

*Correspondence:
Vikas Chaudhary
dr_vikaschaudhary@yahoo.com
Full list of author information is available at the end of the article

Keywords Bacterial infection, Children, High-resolution computed tomography, HIV/AIDS, Pneumocystis jiroveci pneumonia, Pulmonary tuberculosis, Radiological patterns

Introduction

Children with human immunodeficiency virus (HIV) infection frequently present with a wide spectrum of pulmonary complications including the opportunistic infections and neoplasms of the lung that may be associated with high mortality and morbidity. According to world health organization (WHO), an estimated 1.5 million children aged 0–14 years were living with HIV at the end of 2022, and 130 000 children were newly infected in 2022 1. Without access to testing and treatment, 50% of children with HIV die by the age of 2, and 80% do not live to their fifth birthday 2. Most of the children are infected with HIV after vertical transmission from their mother, and majority develop acquired immunodeficiency syndrome (AIDS) early in life. 3

Chest radiograph is the initial imaging modality for evaluation of HIV patients with suspected pulmonary disease. It provides a radiological baseline before initiation of antiretroviral therapy and to monitor treatment response 4, 5. However, 5–10% patients with AIDS and pulmonary disease may have normal or nonspecific radiographic findings. High-resolution CT is more sensitive than radiography for revealing parenchymal abnormalities. CT reveals pulmonary parenchymal and interstitial changes before they are evident on chest radiographs. Also, better delineation and characterization of both localized & diffuse parenchymal abnormalities and lesser inter-observer variation are the definite advantages of CT over chest radiography.

The pulmonary complications of HIV infection are closely related to the degree of immunosuppression which can be predicted by the CD4 lymphocyte count. The absolute CD4 lymphocyte count correlates well with the onset and manifestation of clinical AIDS. 6

In most patients with AIDS, a confident diagnosis of pulmonary complications can be made in combination with clinico-radiological findings, laboratory data, cytohistopathology report and follow-up imaging.

Studies on radiological spectrum of the chest diseases in HIV-infected patients have been done mostly on the western population and cannot be applied directly to other populations due to variation in target population and epidemiology of various infections. Moreover, very limited studies have been done in pediatric patients.

Aims

To study the radiological patterns of chest infections in HIV-infected children and to correlate the radiological findings with CD4 cell count & final diagnosis.

Subjects and methods

The study population comprised of 45 HIV-infected children (1–18 years of age) with chest infections suspected clinically or by chest radiograph (CXR). Demographic data of the patients, their presenting complaints and clinical examination findings were noted. The baseline and most recent CD4 counts were recorded for each patient.

CXR was obtained in all the patients, and MDCT chest (using pediatric protocol on Philips Brilliance 40 CT scanner) was carried out in 27 (60%) out of 45 cases. Decision to do CT chest in selected cases was governed primarily by clinical and laboratory findings where despite treatment children showed inadequate/poor clinical and radiographic improvement or worsening of laboratory parameters. CT was also done in excluding lung disease when the radiographic findings were equivocal and in confirming the presence of clinically suspected disease in patients when chest radiographs were normal.

Chest radiographs and MDCT chest scans were evaluated for:

(i) Any parenchymal, mediastinal, pleural and/or chest wall lesion(s)
(ii) Pattern of parenchymal abnormalities like consolidation, nodule, cavity, cyst, ground-glass opacity (GGO), infiltration, interstitial opacity, mass, etc.
(iii) Distribution of parenchymal abnormalities
(iv) Any other associated finding

Imaging findings were evaluated to arrive at a probable radiological diagnosis.

Imaging findings were correlated with:

(i) CD4 count range for disease spectrum
(ii) Mantoux test, sputum/gastric aspirate examination, blood culture, bronchoscopy and BAL cytology/culture
(iii) Cytohistopathology (biopsy/FNAC)

Microbiological isolation of pathological organism from the sputum/gastric aspirates/bronchoalveolar lavage (BAL)/blood sample was taken as gold standard test to reach a definitive diagnosis. However, there were some limitations to this. Sputum is inadequately produced by children especially in early years of life and they tend to swallow it, children were sometimes on antibiotic treatment for some other co-existing illness which reduced yield from samples, bronchoscopy could not be performed in children who were very sick or had significant cardiopulmonary compromise. In these cases,

microbiological diagnosis was reached on basis of clinical findings, CD4 count levels and most importantly on basis of clinical and radiological improvement to antibacterial/antitubercular/antifungal antibiotic treatment.

The final etiopathological diagnosis was achieved in combination with clinico-radiological findings, laboratory data, cytohistopathology and follow-up imaging.

Statistical evaluation was done using appropriate software (SPSS ver.12). Results were expressed as proportions and Chi-square test was applied to find out statistical significance.

Results

Out of 45 children confirmed to be HIV-infected, 27 (60%) had bacterial infection, 14 (31.11%) had tuberculosis, and four (8.89%) had fungal infection.

The results are presented in the form of tables (Tables 1, 2, 3, 4, 5, 6, 7, 8, 9).

In 27 patients with final diagnosis of bacterial infection (Table 1), chest radiograph suggested

correct diagnosis in 26 patients; however, one patient was misdiagnosed as tuberculosis (with miliary nodules, some of them showing calcification). Chest X-ray and CT combined gave correct diagnosis in all 16 cases where CT was done. CT chest was not done for the case misdiagnosed as tuberculosis on chest X-ray. However, this patient had presented with fever and productive cough for 5 days and had past history of pulmonary tuberculosis. Sputum sample of this patient isolated pseudomonas, so patient was correctly diagnosed as a case of bacterial infection on combining imaging, clinical and laboratory findings.

In patients with final diagnosis of tubercular infection (Table 2), out of 14 cases, four were correctly diagnosed on chest X-ray, whereas 10 were misdiagnosed (one patient had normal chest X-ray and nine other cases were misdiagnosed as bacterial infections). With chest X-ray and CT combined (done in 11 patients), correct diagnosis was given in eight patients, whereas three patients were wrongly diagnosed as bacterial infections. On combining imaging and clinical criteria, 12 patients were correctly diagnosed as tuberculosis. Out of remaining two cases, one patient had Mantoux test positive and second patient isolated Mycobacterium tuberculosis in BAL and these were then correctly diagnosed as tuberculosis.

In patients with final diagnosis of fungal infection (Table 3), two out of four patients were diagnosed correctly on chest X-ray; however, one patient with consolidation without LNs was misdiagnosed as bacterial infection, and another one had normal chest X-ray.

Table 1 Imaging assessment in patients with final diagnosis of bacterial infection

Imaging assessment (with & without clinical & laboratory assessment)	Imaging diagnosis of bacterial infection ($n=27$)	
	Correct diagnosis	Misdiagnosis
Chest X-ray (done in all 27 patients) (consolidation, collapse, no LNs)	26	1 (TB-miliary nodules)
Chest X-ray + CT (done in 16 patients) (consolidation, collapse, with/without LAP, no lymph nodal necrosis)	16	0
Imaging + clinical (acute presentation < 1 week, fever with productive cough)	27	0
Imaging + clinical + laboratory findings	27	0

TB tuberculosis

Table 2 Imaging assessment in patients with final diagnosis of tubercular infection

Imaging assessment (with & without clinical & laboratory assessment)	Tubercular infection ($n=14$)	
	Correct diagnosis	Misdiagnosis
Chest X-ray (done in all 14 patients) (hilar &/or mediastinal LNs with/without parenchymal lesions, miliary nodules)	4	1-normal CXR 9-bacterial (consolidation)
Chest X-ray + CT (done in 11 patients) (necrotic LNs with/without parenchymal lesions, miliary nodules)	8	3-bacterial (consolidation, with/without LNs)
Imaging + clinical (chronic symptom > 3 weeks, fever with cough)	12	2-bacterial (BAL isolated MTB in one patient & Mantoux test was positive in another patient)
Imaging + clinical + laboratory findings	14	0

GGO Ground-glass opacification, *BAL* Broncho-alveolar lavage, *MTB Mycobacterium tuberculosis*

Table 3 Imaging assessment in patients with final diagnosis of fungal infection

Imaging assessment (with & without clinical & laboratory assessment)	Fungal infection ($n=4$)	
	Correct diagnosis	Misdiagnosis
Chest X-ray (done in all 4 patients) (diffuse GGO/haziness)	2	1-normal CXR 1-bacterial (consolidation, no enlarged LN)
Chest X-ray + CT (done in 3 patients) (diffuse GGO with crazy paving)	3	0
Imaging + clinical (hypoxia, no response to antibacterial or antitubercular drugs)	4	0
Imaging + clinical + laboratory findings	4	0

GGO Ground-glass opacification, *LN* Lymph node

Table 4 Imaging pointers to specific etiology

Imaging pointers or markers to infective association	Whether the association is statistically significant (i.e., *P* value < 0.05)	Sensitivity (%)	Specificity (%)
Chest radiograph (CXR) findings as markers			
Consolidation and bacterial infection	YES	**88.89**	44.44
Bronchiectasis and bacterial infection	No	29.63	88.89
Focal GGO/haziness and bacterial infection	No	18.52	61.11
Mediastinal/hilar LAP and tuberculosis	YES	21.43	**100**
Diffuse GGO/haziness and fungal infection	YES	50	**100**
Chest CT findings as markers			
Consolidation and bacterial infection	YES	**93.75**	35.71
Bronchiectasis and bacterial infection	No	56.25	78.57
Focal GGO and bacterial infection	No	31.25	57.14
Mediastinal/hilar LAP and tuberculosis	YES	**90.91**	**73.68**
Necrotic mediastinal/hilar LAP and tuberculosis	YES	**72.73**	**100**
Calcified mediastinal/hilar LNs and tuberculosis	No	18.18	**89.47**
Diffuse GGO and fungal infection	YES	**100**	**100**

GGO Ground-glass opacification, *LAP* Lymphadenopathy, *LNs* Lymph nodes

Table 5 Correlation of CD4 count with type of pulmonary infection

Pulmonary infections	CD4 count (cells/mm^3)		
	< 200	200–500	> 500
Bacterial ($n=27$)	2	12	13
Tubercular ($n=14$)	2	10	2
Fungal ($n=4$)	4	–	–

In one patient with normal X-ray, CT chest was done which showed features of PJP infection, not well seen on radiograph. In another patient, wrongly diagnosed as bacterial infection on chest X-ray, CT chest was not done. This patient had cough and fever, and did not show any improvement in spite of antibacterial antibiotics for 3 weeks. Sputum sample isolated Candida species, thereby correctly diagnosing it as fungal infection.

As expected, CT had higher sensitivity in all types of infections as compared to chest X-ray (100% for bacterial and fungal infections and 72.73% for tuberculosis). With a holistic approach, i.e., after combination of imaging, clinical and laboratory findings, the sensitivity improved to 100% in all types of infections.

The results indicate that imaging diagnosis of consolidation on CXR or CT in HIV-infected children should suggest possibility of bacterial etiology (*P* value < *0.05*), whereas tubercular etiology is to be considered in patients with imaging findings of mediastinal/hilar lymphadenopathy (with or without necrosis)

Table 6 Immunological status of study participants in accordance to CD4 count

Immunological status	Bacterial ($n=27$)	Tubercular ($n=14$)	Fungal ($n=4$)	Total ($n=45$) (%)
No immunosuppression (CD4 count ≥ 25% of total lymphocytes)	12	1	0	13 (28.89)
Moderate immunosuppression (CD4 count ≥ 15 to < 25% of total lymphocytes)	11	10	0	21 (46.67)
Severe immunosuppression (CD4 count < 15% of total lymphocytes)	4	3	4	11 (24.44)

Table 7 CD4 count and antiretroviral therapy (ART) status of the study participants (patients)

CD4 cell Count (cells/mm^3)	Bacterial (n = 27)		Tubercular ($n=14$)		Fungal ($n=4$)	
	ART	Pre-ART	ART	Pre-ART	ART	Pre-ART
< 100	0	1	0	0	0	0
100–200	0	1	2	0	2	2
> 200–500	7	5	8	2	0	0
> 500	11	2	0	2	0	0
Total	18	9	10	4	2	2

Thirty (66.67%) out of 45 patients were on ART and 15 (33.33%) patients had not received ART. Patients receiving ART had better CD4 counts as compared to patients not receiving ART (pre-ART patients)

Table 8 Duration of ART in respect of the study participants receiving ART

Duration of ART	No. of patients ($n=30$)
< 1 year	10
1–3 year	12
> 3 year	8
Total	30

ART Antiretroviral therapy

(P value < *0.05*). Further, when diffuse GGO/haziness is seen on CXR/CT, it should be suggestive of fungal etiology (P value < 0.05) (Table 4).

The present study also showed that bacterial infections have a tendency to occur in early HIV infection with relatively preserved immune system. On the other hand, tubercular infections usually occur in moderate immunosuppression, and fungal infections should be expected in patients with severe immunosuppression (Tables 5,6).

Thirty (66.67%) out of 45 patients were on ART and 15 (33.33%) patients had not received ARM (pre-ART patients). Patients receiving ART had better CD4 counts as compared to patients not receiving ART (Table 7).

Twenty patients (66.7%) had been receiving ART for more than a year and 10 patients (33.3%) had received ART for less than a year (Table 8).

No microorganism could be isolated in 35 cases (77.8%) (sputum/gastric aspirate/BAL/blood culture) (Table 9). Nine cases (20%) had monomicrobial infection (four bacterial, three tubercular, two fungal). Among four cases of bacterial infection, sputum isolated pneumococcus and pseudomonas in one case each, BAL isolated Klebsiella and pneumococcus in one case each. Out of three tubercular cases, BAL isolated Mycobacterium tuberculosis in one case and MDR-TB in two cases with no isolation of

Table 9 Microbial isolation of different species

Mono/polymicrobial infections	Bacterial ($n=27$)	Tubercular ($n=14$)	Fungal ($n=4$)	Total No. (%)
Monomicrobial	4	3	2	9 (20)
Polymicrobial	0	0	1	1 (2.2)
No microorganism isolated	23	11	1	35 (77.8)

other microorganisms in sputum/gastric aspirate/blood culture (suggestive of monomicrobial infection). In two fungal cases, sputum isolated Candida species.

One patient with fungal infection had both candida and PJP isolated in BAL sample.

Discussion

India had around 21 lakh people living with HIV in 2017, among whom 56% were accessing antiretroviral therapy 7. The development of highly active antiretroviral therapy (HAART) and prophylaxis therapy for opportunistic infections has significantly decreased the viral load (and thus HIV related morbidity and mortality) in adults as well as in pediatric populations. However, pulmonary infections remain the first cause of hospital admission in HIV-infected children even in the HAART era. 5

In present study, majority of children (51.11%) were in age group > 10 years to 15 years, 22.22% were between 5 and 10 years, 17.78% were < 5 years, and 8.89% were > 15–18 years of age. The male to female ratio was 2.75:1.

Pulmonary manifestations, viz. fever & cough, were seen in 95.56% of the patients at time of presentation.

In present study, 30 (66.67%) out of 45 patients were on ART and 15 (33.33%) patients did not receive ART (Table 8). It was observed that the patients receiving ART had better CD4 counts as compared to patients not receiving ART (pre-ART patients).

Bacterial infections (Figs. 1, 2, 3, 4, 5, 6, 7, 8)

A total of 27 (60%) out of 45 patients were diagnosed with bacterial infections in our study (Table 1). Similar increased incidence of bacterial pneumonia has been reported by *Afessa* et al. (42% in an autopsy series of 233 HIV-infected individuals) and supported by others. 8, 9

Fever, productive cough & tachypnea were the most common presenting complaints, followed by breathlessness and chest pain.

In the present study, microorganisms isolated in four (8.89%) patients were *Pneumococcus, Staphylococcus, Pseudomonas and Klebsiella.* In 23 patients, no microorganism could be isolated in sputum/BAL/gastric aspirate/blood culture. They were diagnosed as probable

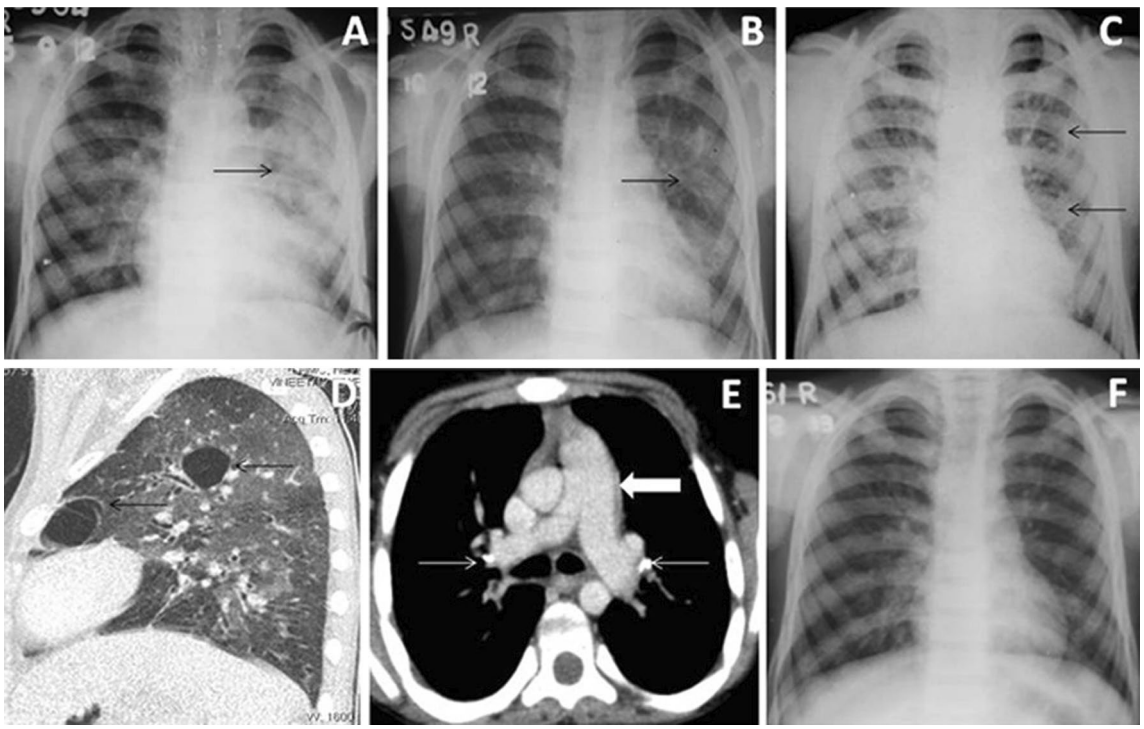

Fig.1 Bacterial Infection. Frontal chest radiograph (CXR) in a 12-year-old HIV-positive male reveals diffuse consolidation (arrow in **A**) involving left lung field. After start of antibiotics, the consolidation showed gradual resolution (arrow in **B**), with appearance of two oval cystic lucencies (arrows in **C**) in left upper & mid zones suggesting pneumatocele formation. CT chest (sagittal plane in lung window) confirmed presence of pneumatoceles in left upper lobe (arrows in **D**). Axial CT in soft tissue window (**E**) showed enlarged pulmonary artery (thick arrow) suggestive of pulmonary hypertension, and few calcified mediastinal/hilar lymph nodes (thin arrows). Patient's CD4 count was 354 cells/cu.mm. Sputum isolated pneumococcus. Patient showed complete clinical and radiological improvement after a course of antibiotic with non-visualization of pneumatoceles on follow-up CXR (**F**)

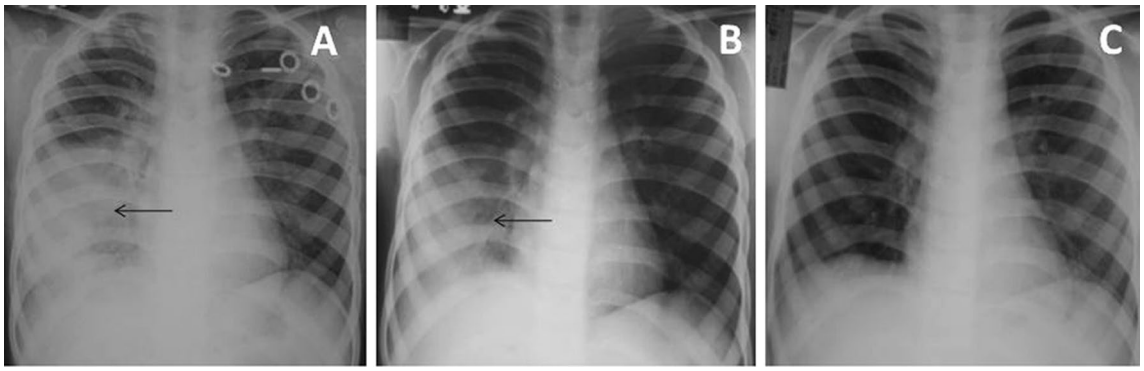

Fig. 2 Bacterial Infection. Frontal CXR in a 13-year-old HIV-positive female shows right lower lobe consolidation involving mid and lower zones, causing silhouetting of adjacent right hemi-diaphragm (arrows in **A** & **B**). Sputum could not isolate any microorganism. CD4 count was 301 cells/cu.mm. Patient was put on antibacterial antibiotics and improved clinically & radiologically (**C**) over a period of 4 weeks

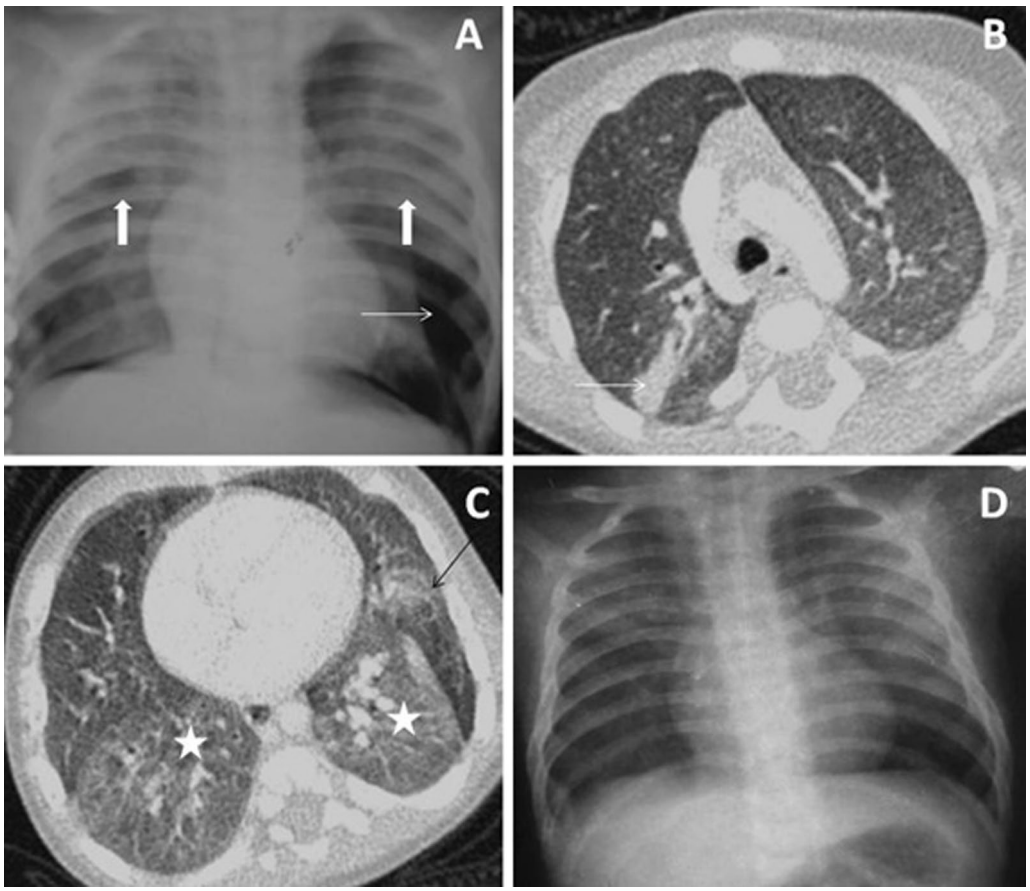

Fig. 3 Bacterial Infection. An 18-month-old male child reveals consolidation/haziness in bilateral upper & mid zones (thick vertical arrows), with hyperinflation in left lower zone (thin horizontal arrow), on frontal CXR (**A**). CT chest (axial, lung window) shows subsegmental consolidation in RUL (arrow in **B**), GGO in bilateral lower lobes (asterisks) and consolidation with hyperinflation of lateral basal segment of LLL (arrow in **C**). Sputum could not isolate any microorganism. BAL isolated *Klebsiella* species. CD4 count was 406 cells/cu.mm. Patient responded to antibacterial antibiotics and improved clinically & radiologically (**D**) over a period of 4 weeks

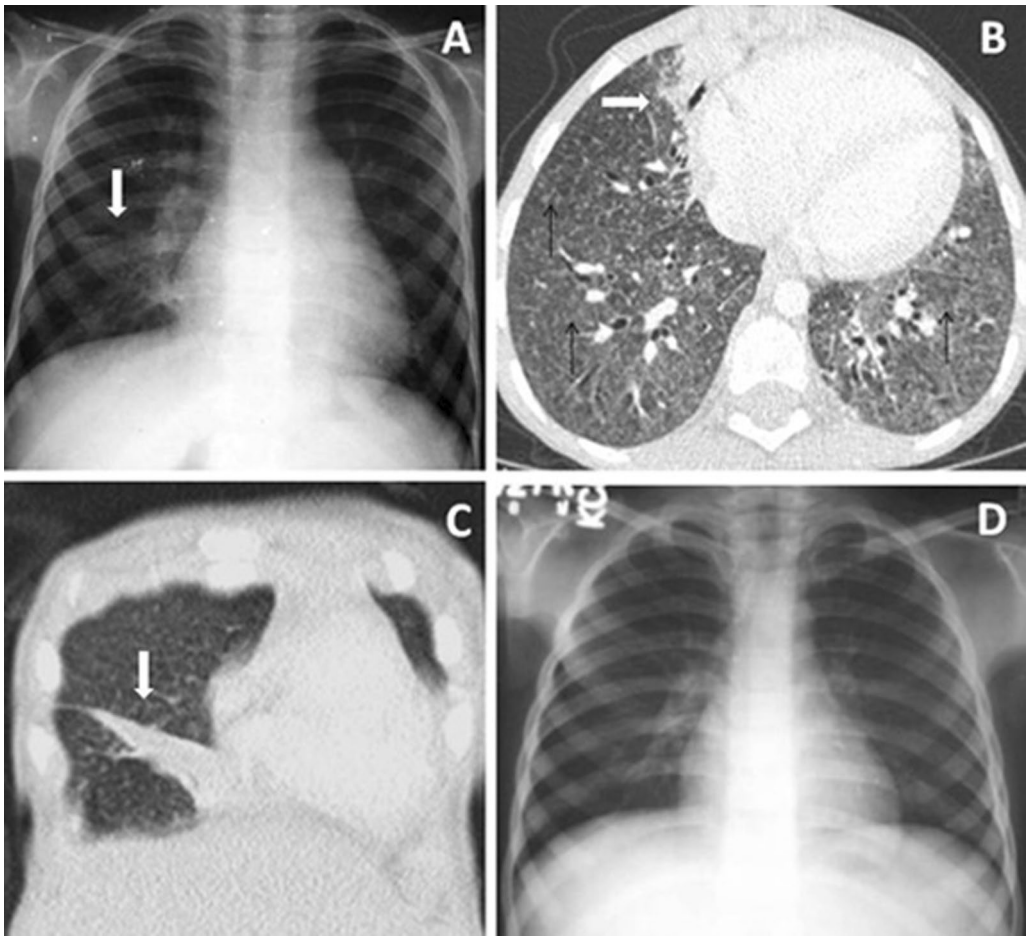

Fig. 4 Bacterial Infection. CXR (PA view) in a 12-year-old HIV-positive child reveals inhomogeneous opacity in right para-cardiac region (arrow in **A**). CT chest (lung window) shows presence of consolidation (white arrow in **B**) in medial segment of RML, along with centrilobular nodules (black arrows in **B**) in bilateral lung fields on axial image, and collapse of anterior segment of RUL on sagittal image (arrow in **C**). Sputum could not isolate any microorganism. CD4 count was 400 cells/cu.mm. Patient was given antibacterial antibiotics and improved clinically & radiologically (**D**) over a period of 3 weeks

bacterial patients on the basis of clinical and radiological findings and all of them showed clinical and radiological improvement with antibacterial antibiotics.

Thirteen (48.15%) out of 27 patients had CD4 count > 500 cells/mm^3, 12 (44.44%) patients had CD4 count > 200–500 cells/mm^3, and only two patients had CD4 count < 200 cells/mm^3 (Table 5). The present study observed that bacterial infections tend to occur in early stages of HIV infection when immune status is relatively preserved. *Hirschtick* et al. described similar correlation of CD4 count with bacterial infections. They stated that although bacterial pneumonia often occurs in early stages of HIV infection, the risk of bacterial infection increases steadily with declining CD4 lymphocyte counts. 9

Eighteen (66.67%) out of 27 patients with bacterial infection were on ART (Table 7), and 11 (61.11%) of these had CD4 count > 500 cells/mm^3, and 38.89% had CD4 count in the range of 200–500 cells/mm^3 suggesting better immune status of patients on ART with bacterial infections. In comparison with this, seven out of nine patients (i.e., 77.78%) of bacterial infection not receiving ART had CD4 counts of 500 cells/mm^3 or less.

CXR was done in all 27 (100%) patients, while CT chest was done in 16 (59.26%) patients (Table 1). On CXR, consolidation (Figs. 1, 2, 3, 4, 5, 6, 7, 8) was the most common finding, seen in 24 (88.89%) patients, being predominantly focal in 20 patients and diffuse in four patients. *Boiselle* et al. also observed the presence of focal

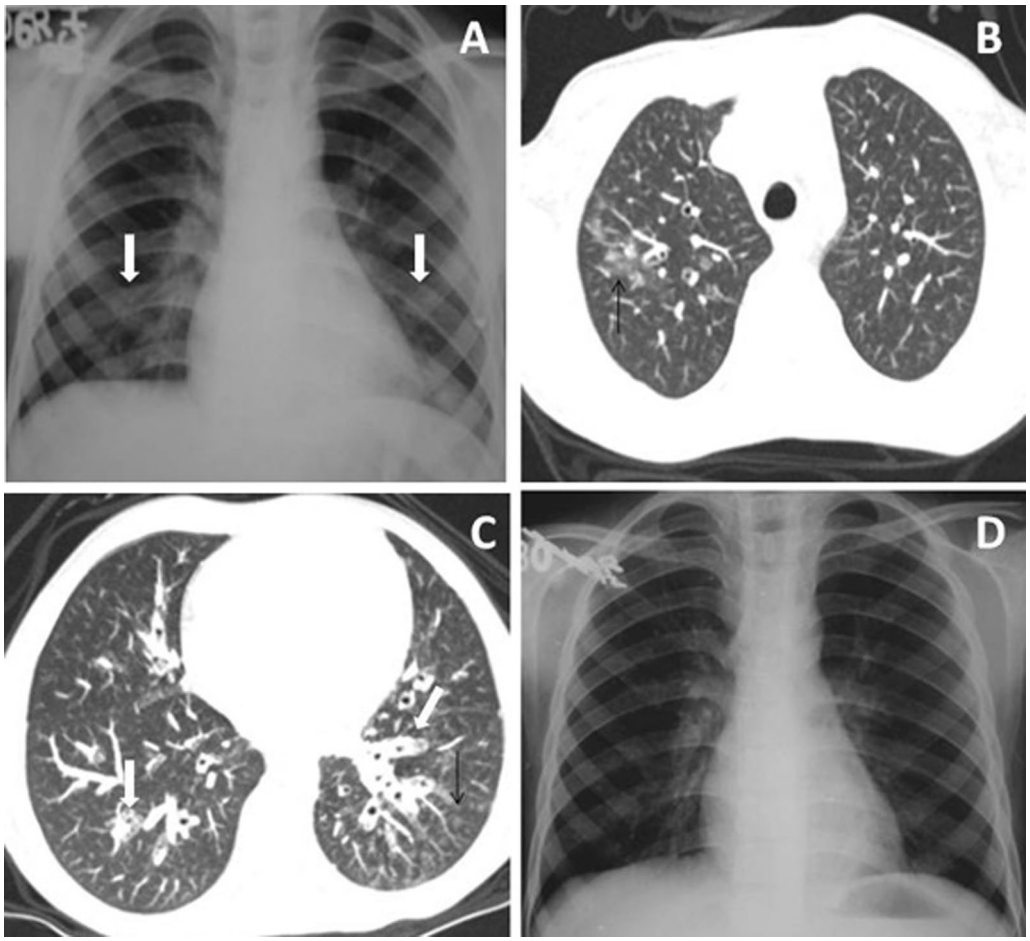

Fig. 5 Bacterial Infection. A 10-year-old male, presented with cough and fever since last 2 days. Chest X-ray (PA view) reveals bilateral LZ haziness (arrows) (**A**). CT chest (axial view) shows subsegmental GGO in RUL (arrow) (**B**) and nodular air-space opacity in LLL (black arrow) along with bronchiectatic changes and peribronchial thickening in B/L LL (white arrows) (**C**). Sputum could not isolate any microorganism. CD4 count was 95 cells/cu.mm. Patient was given antibacterial antibiotics and improved clinically and radiologically (**D**) over a period of 4 weeks

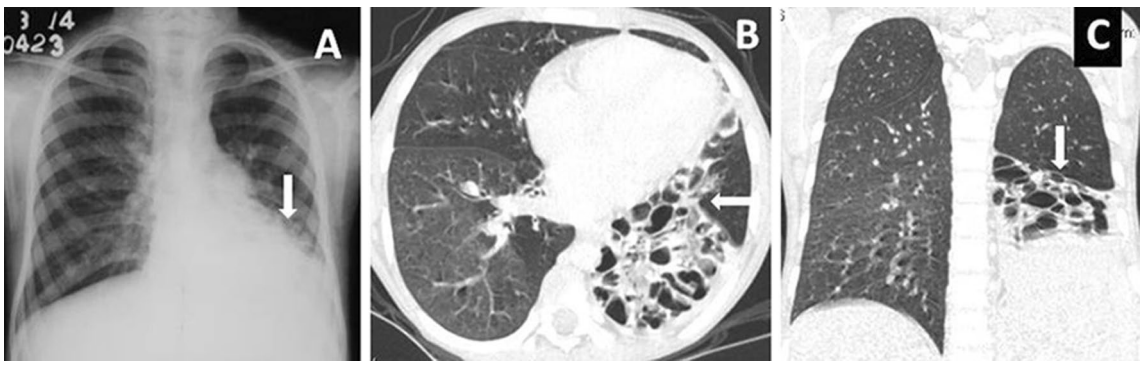

Fig. 6 Bacterial Infection. An 11-year-old-HIV-positive male patient presented with cough & fever since 15 days. CXR-posteroanterior (PA) view reveals a homogenous opacity involving left lower zone causing silhouetting of left cardiac border and left hemi-diaphragm (arrow, **A**). CT chest shows left lower lobe and lingular atelecto-bronchiectatic changes (arrow in **B**,**C**) with ipsilateral mediastinal shift and upward displacement of the left hemi-diaphragm. Sputum could not isolate any microorganism. CD4 count was 248 cells/cu.mm. Patient was given antibacterial antibiotics and improved clinically over a period of 2 weeks

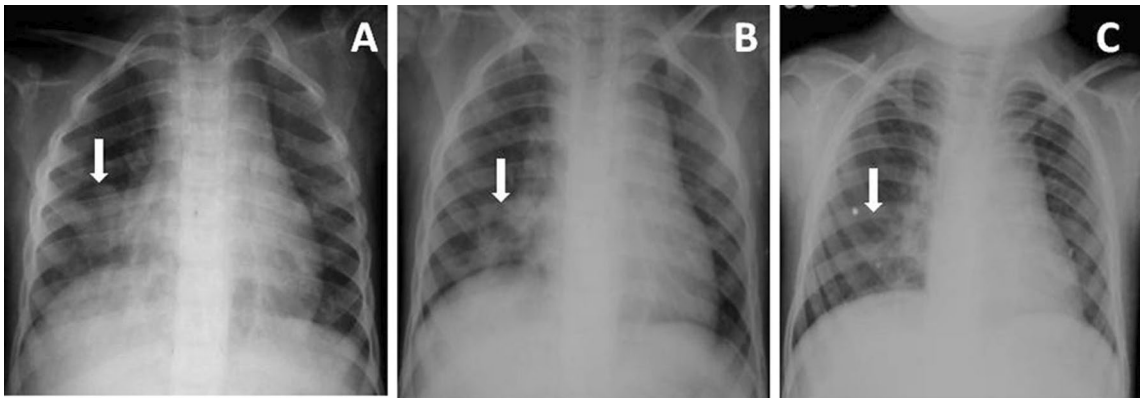

Fig. 7 Bacterial Infection. Frontal CXR in a 6-year-old HIV-positive female reveals focal area of consolidation in right para-cardiac region (arrow, **A**), later progressing into frank cavitation (arrow, **B**). Sputum could not isolate any microorganism. CD4 count was 400 cells/cu.mm. Patient was given antibacterial antibiotics and improved clinically and radiologically (**C**) over a period of 4 weeks

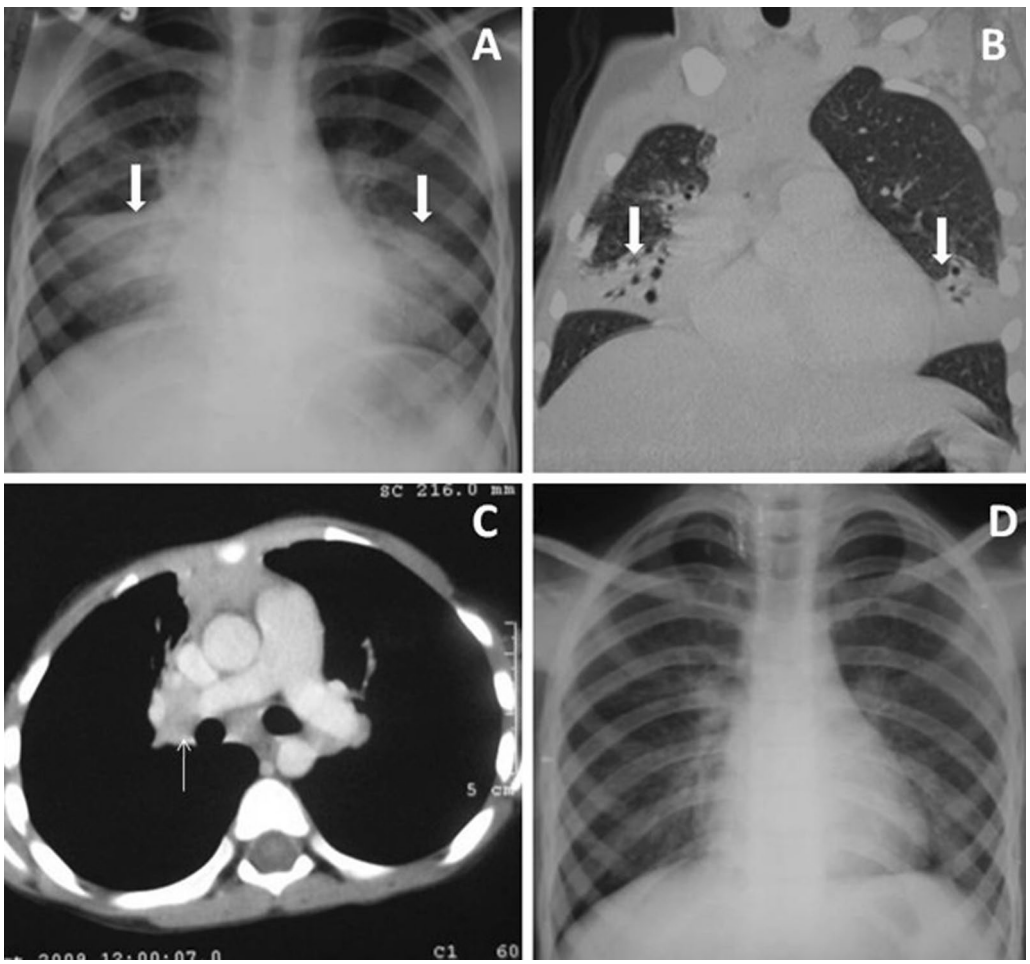

Fig. 8 Bacterial Infection. CXR-PA view in a 13-year-old HIV-positive female shows bilateral mid-zone triangular patchy opacities causing silhouetting of adjacent cardiac borders (arrows, **A**). CT chest shows right middle lobe (RML) and lingular atelecto-brochiectatic changes (arrows in **B**, lung window), and mediastinal lymphadenopathy (arrow in **C**, soft issue window). Sputum could not isolate any microorganism. CD4 count was 1001cells/cu.mm. Patient was given antibacterial antibiotics and improved clinically and radiologically (**D**) over a period of 4 weeks

consolidation on CXR in 45–60% patients with bacterial pneumonia 13. The focal segmental/subsegmental consolidation was seen in 15 (93.75%) out of 16 patients in our study in whom CT scan was done. Focal segmental consolidation, usually associated with bacterial infection, was also observed by *Sider* et al. in their study. 10

Bacterial pneumonia may also present as solitary or multiple pulmonary nodules. Nodular air-space opacities were observed as ill-defined lesions ranging from 1 to 3 cm in size in four (14.81%) out of 27 patients on CXR. Besides these, in six (37.5%) out of 16 patients, CT chest was able to diagnose smaller opacities (micronodules) ranging from 3 mm to 1 cm size that were beyond the resolution of CXR. *Jasmer* et al. reported bacterial pneumonia to be the most important cause of pulmonary nodules followed by tuberculosis in HIV-infected patients. 11

Cavitation within consolidation was observed in two (7.41%) patients which resolved with antibiotics on follow-up CXR. Cavitary pulmonary lesions are often associated with bacterial pneumonia in HIV-infected patients, confirmed by *Aviram* et al. in 85% patients. 12

CXR did not show any hilar or mediastinal lymphadenopathy (LAP). CT scan done in 16 patients revealed hilar LAP (Fig. 8) in two (12.5%) patients and mediastinal LAP in five (31.25%) patients. Calcification was seen in one hilar and one mediastinal lymph node; however, no necrosis was evident. This is supported by *Boiselle* et al. observation that although intrathoracic lymph node enlargement is usually not evident on CXR, mildly enlarged nodes are frequently seen on CT scans of patients with bacterial pneumonia. 13

CT scan done in 16 patients revealed subsegmental collapse in three (18.75%) patients and lobar collapse in one (6.25%) patient (Fig. 4, 8). Paraseptal emphysema was seen in two (12.5%) patients and pneumatocele in one (6.25%) patient (Fig. 1). Pulmonary arterial hypertension (PAH) was also detected in one (6.25%) (Fig. 1) patient having enlarged pulmonary artery segment with distal pruning of vessels later confirmed on echocardiography.

Tubercular infection (Figures 9, 10, 11, 12, 13, 14, 15)

The prevalence of tuberculosis as opportunistic infection in HIV-infected children has been reported as 11–40% in various series. Pulmonary tuberculosis was reported in 32–60% patients and extrapulmonary (abdominal, CNS, disseminated) tuberculosis in 7–45% patients. [13–15

The present study, conducted on HIV-infected Indian children with chest manifestations, diagnosed 14 patients with pulmonary tuberculosis. *Mycobacterium* could be isolated only in three out of 14 patients from BAL specimen. Of these three patients, one had Mantoux negative tuberculosis, while other two had Mantoux positive multi-drug resistant tuberculosis (MDR-TB). Hence, our study detected MDR-TB in two (14.29%) out of the 14 patients as compared to five (5.4%) out of 93% patients as reported by *Hessling* et al.16 In 11 patients, no mycobacterium could be isolated in sputum/BAL/gastric aspirate. Six of these patients were Mantoux positive and showed radiological evidence of tuberculosis in the form of necrotic mediatinal/hilar lymph nodes with/without

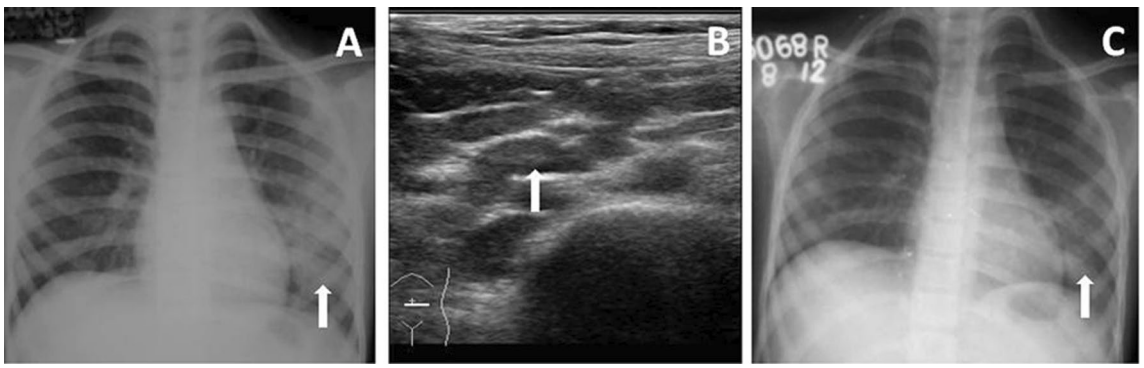

Fig. 9 Tubercular Infection. Frontal chest radiograph in a 9-year-old HIV-positive male demonstrates confluent ill-defined nodular air-space opacities involving left lower zone (arrow, **A**). Ultrasound abdomen shows multiple mesenteric & retroperitoneal lymph nodes (arrow, **B**), some of which showed conglomeration and necrosis. His CD4 count was 256 cells/cu.mm, and Mantoux was strongly positive. Sputum could not isolate any microbe. On the basis of combined clinico-radiological findings, positive Mantoux test and CD4 count, antitubercular therapy (ATT) was started and patient improved both clinically and radiologically, showing complete resolution of the lesion (arrow, **C**)

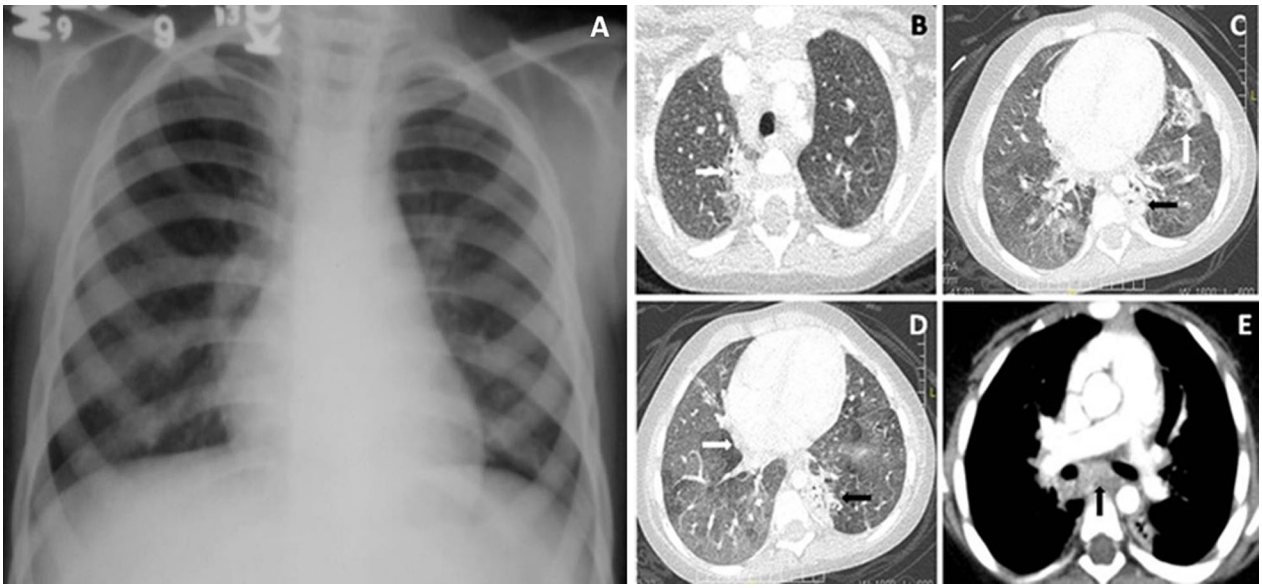

Fig. 10 Tubercular Infection. A 13-year-old HIV-positive male presented with fever of 2 weeks' duration. Frontal chest radiograph (**A**) was normal. CT chest (axial view, lung window) revealed patchy areas of consolidation & ground-glass opacity in bilateral lung parenchyma (arrow in **B**,**C**,**D**). Conglomerate, mildly enhancing mediastinal lymph nodes were noted in subcarinal location (arrow, **E**) on mediastinal window. Patient's CD4 count was 425 cells/cu.mm. BAL isolated *Mycobacterium*, and Mantoux test was positive. Patient started on ATT on the basis of these findings and showed significant clinical improvement

parenchymal lesion. All these 11 patients diagnosed as tuberculosis showed clinical and radiological improvement with antitubercular treatment (ATT).

Positive Mantoux test in eight (57.14%) out of 14 patients suggests that in early HIV disease tuberculin skin test is usually positive; however, as the degree of immunosuppression progresses, only 20–40% may demonstrate a positive skin test for tuberculosis. 15

In present study, eight (80%) out of 10 patients on ART and two patients with pre-ART status had CD4 counts > 200–500 cells/mm^3, whereas two (20%) patients on ART had CD4 count < 200cells/mm^3, and two patients with pre-ART status had CD4 count > 500 cells/mm^3. Thus, it is observed that tuberculosis is common in HIV children with CD4 count in the range of 200–500 cells/mm^3 (Table 5, 7).

The sputum positivity in HIV patients ranges from 15.4 to 85% depending on immune status of the patients. Chance of acid-fast bacillus (AFB) isolation remains high in patients with mild immunosuppression compared to those with advanced disease. Highly immunosuppressed patients have only subacute symptoms and infected with lower colony count of *M. tuberculosis*, and hence, the diagnosis may be more difficult in immunosuppressed than in immunocompetent patients.

CXR was done in all 14 (100%) patients, while CT chest was done in 11 (78.57%) of these patients (Table 2). Radiographic appearance of tuberculosis (TB) in AIDS differs from that in immunocompetent host, having more diffuse and lower zone disease, miliary disease, lymphadenopathy and increased incidence of normal CXR 17, 18. Similar findings have been observed in our study. Parenchymal abnormality was seen in 10 (71.43%) patients. Out of these, six patients showed predominantly middle & lower zone involvement and only one patient had predominantly upper & mid-zone involvement. Diffuse involvement was seen in three patients.

Endobronchial tuberculosis manifests as normal chest X-ray and has been observed in 15% patients with tuberculosis by Leung et al. 18 The air-space nodular lesions, especially centrilobular opacities, characteristic of endobronchial spread of tuberculosis are usually better picked up on CT due to inherent spatial resolution of CT as compared to CXR. In present study, three patients with normal CXR had conglomerate/necrotic mediastinal/hilar lymph nodes, and one patient with normal CXR had endobronchial tuberculosis evident as multiple ill-defined nodular air-space opacities (3 mm–1 cm size), centrilobular distribution and focal GGO in right upper lobe on CT scan (Fig. 13).

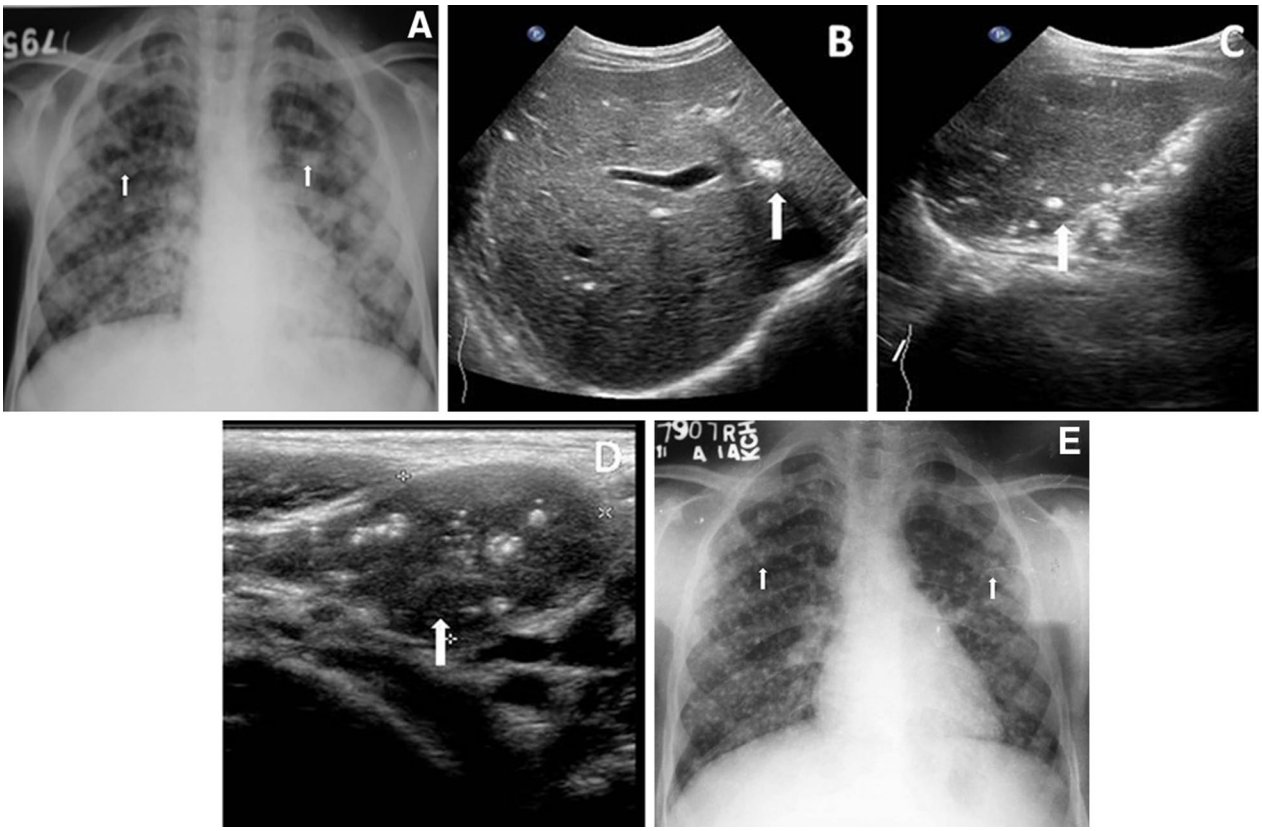

Figure 11 Tubercular Infection. Frontal chest radiograph in a 14-year-old male, a K/C/O HIV/AIDS, reveals diffuse ill-defined nodular air-space opacities throughout bilateral lung fields (arrows, **A**), few of them showing areas of confluence and calcification. Ultrasound abdomen in same patient shows calcified granulomas in liver (arrow, **B**), spleen (arrow, **C**) and conglomerated mesenteric lymph nodes with discrete calcifications (arrow, **D**). Patient's CD4 count was 655 cells/cu.mm. BAL isolated MDR-TB, Mantoux test was positive. Patient was put on ATT on the basis of these findings and showed significant clinical improvement. Follow-up (after 6 months) CXR shows resolution of nodular opacities and presence of multiple calcific lesions in bilateral lungs (arrows, **E**)

On CXR, consolidation was the most common finding, seen in seven (50%) patients, being predominantly focal in six patients and diffuse in one patient. CT done in 11 out of 14 patients showed subsegmental consolidation in seven (63.64%) out of 11 patients (Figs. 8, 12). *Leung* et al.18 , in their study, noted consolidation in 43% patients of HIV-positive patients with pulmonary tuberculosis. Higher percentage noted in our study could be contributed to small sample size and selective inclusion of patients with chest manifestations suspected clinically or on CXR. Cavitation has been reported in HIV patients with tuberculosis having CD4 counts > 200 cells/mm^3. 19 In present study, one (7.14%) patient with CD4 counts 285 cells/mm^3 had cavitation on CECT chest. Centrilobular distribution of nodules was seen in six patients (Figs. 12, 13) with tree-in-bud appearance (Fig. 15) in two of these patients. Nodules size ranged from 1 to 3 cm in four patients and 3 mm–1 cm (micronodules) in two patients. Similar pattern of nodular opacities has been reported by other authors also. 18, 19

On CXR, lymphadenopathy was observed only in three (21.43%) patients, two hilar and one mediastinal in location. Contrast-enhanced CT (CECT) revealed mediastinal lymphadenopathy in eight (72.73%) patients, with central necrosis and rim enhancement seen in six (54.55%) patients. Four of these patients had associated hilar lymphadenopathy on CECT (Figs. 10, 12, 15). Hilar and/or mediastinal lymph nodes with central areas of low attenuation (necrosis) and peripheral rim enhancement on contrast enhanced CT are highly suggestive of active tubercular infection. 18

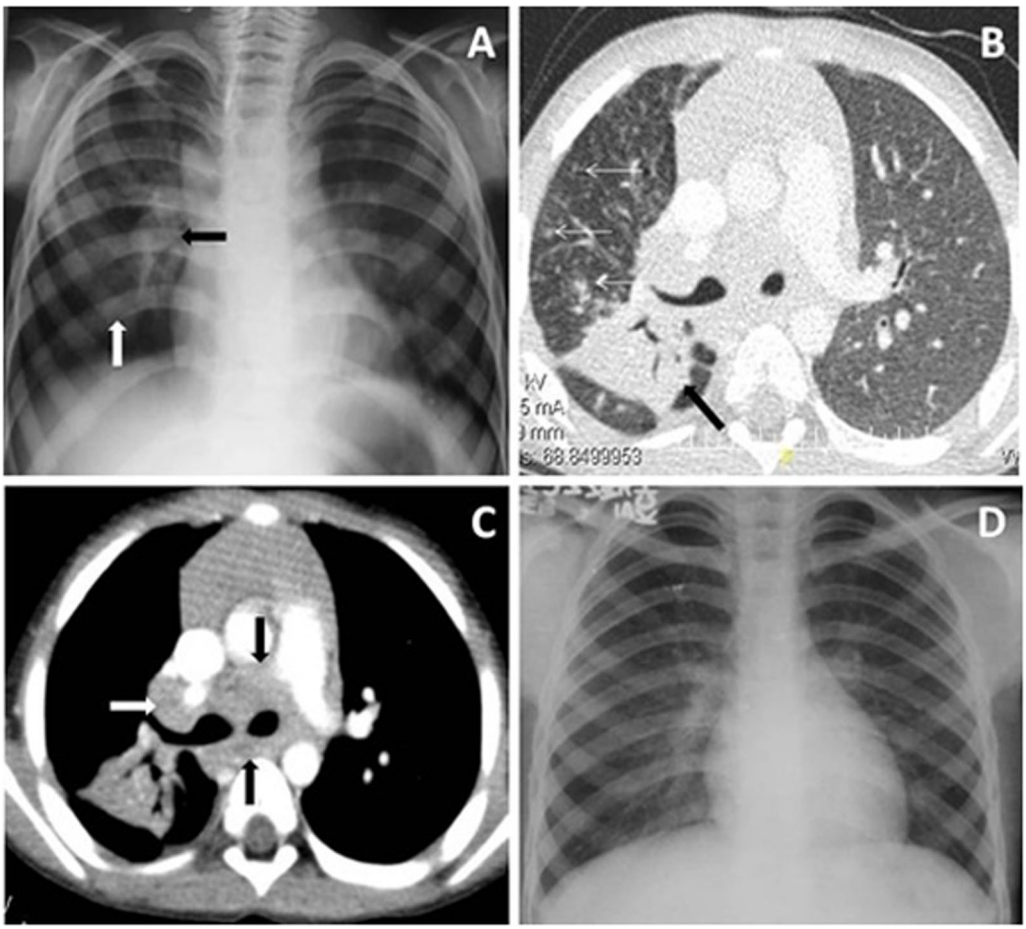

Fig. 12 Tubercular Infection. A 17-year-old HIV-positive female presented with cough & fever for 7 days. CXR shows patchy consolidation (white arrow, A) in right lower zone, and prominent right hilum with lobulated lateral margin (black arrow, **A**). CECT CHEST (axial view) reveals consolidated posterior segment of RUL (black arrow, B), and multiple ill-defined centrilobular nodules in anterior segment of RUL (white arrows, **B**). Precarinal/subcarinal (black arrows, **C**) and right hilar (white arrow in C, just lateral to truncus anterior) lymph nodes, with subtle internal areas of necrosis, are seen on mediastinal window. Patient's Mantoux test was positive. Her CD4 count during this episode was 657 cells/$mm^{3.}$ Sputum and BAL could not isolate any microorganism. On the basis of these findings, ATT was started and patient showed clinical and radiological improvement (**D**) on completion of the therapy

Pleural effusion (Fig. 14) and pulmonary hypertension (Fig. 15) were observed each in one patient, both on CXR and CT scan. Pericardial effusion was detected only on CT scan in one patient. *Leung* et al. detected pleural effusion in 21% of HIV-positive tubercular patients 18. Variation in our study may be due to small study group, differences in severity of infection and host immunity.

Fungal infections (Figures 16, 17, 18)

The introduction of HAART and widespread prophylaxis therapy for opportunistic infections has declined the incidence of *Pneumocystis jiroveci* pneumonia (PJP).

Four (8.89%) out of 45 patients included in this study were diagnosed with fungal infection. Of these, one patient had polymicrobial infection by both Candida and *PJP* isolated from BAL and two had sputum positive Candida infection.

Fever, tachypnoea and breathlessness were common presenting symptoms, seen in three of the four patients. One patient had fever only.

All the four patients with fungal infection were severely immunocompromised having CD4 counts < 200 cells/mm^3 with pre-ART status in two patients and two patients on ART (Table 5, 7). Patients who develop PJP

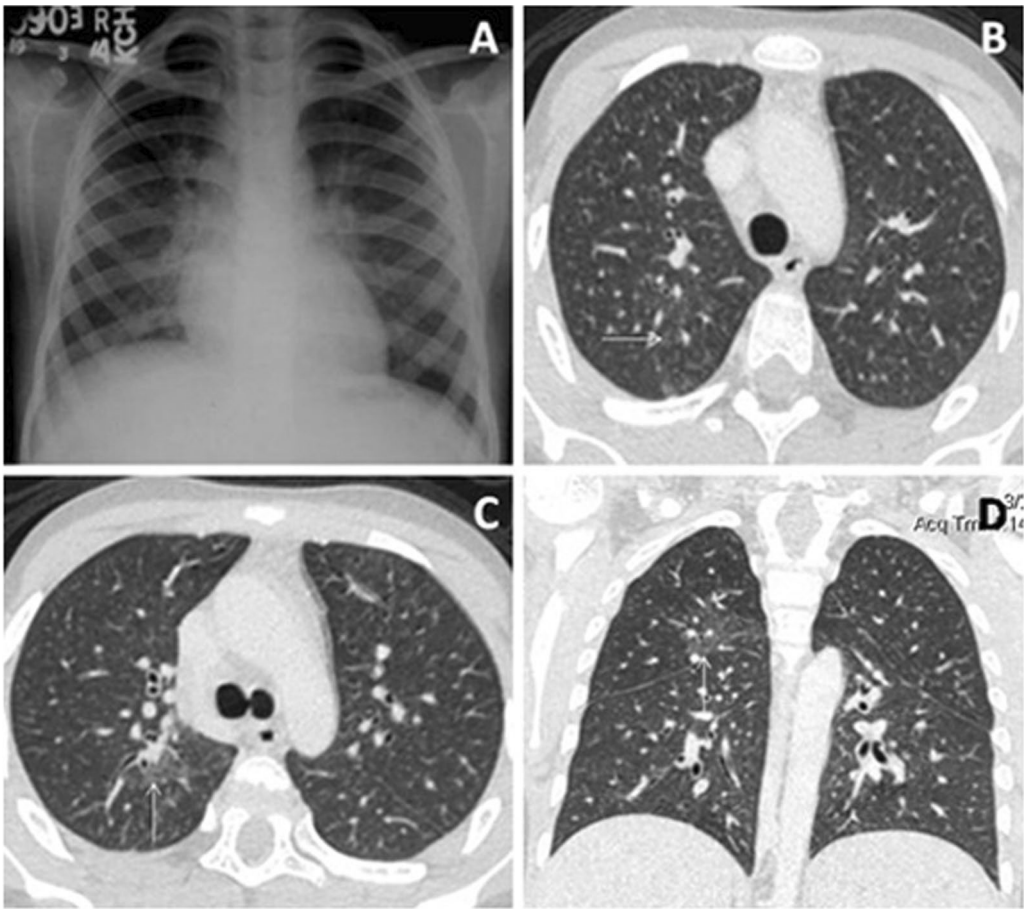

Fig. 13 Tubercular Infection. Chest radiograph (**A**) was normal in this 12-year-old HIV-positive male, who presented with fever since 4 days. CECT chest (**B**,**C**,**D**) was then done, which showed subsegmental area of GGO along with ill-defined centrilobular nodules in RUL, predominantly involving posterior segment (arrows in **B**,**C**). Ultrasound abdomen revealed multiple mesenteric lymph nodes, some of which showed central necrosis (not shown). Sputum could not isolate any microorganism, BAL isolated *Mycobacterium tuberculosis*. CD4 count was 150 cells/cu.mm. On basis of these findings, ATT was started and patient showed clinical improvement within 10 days of start of ATT

infection almost always have CD4 counts < 200 cells/mm^3 as reported by *Morris* et al.20 Young infants with HIV infection are more prone to PJP infection because it follows primary infection with little innate host immunity and immature immune defenses. In older children, PJP infection is caused during more severe immunosuppression.

CXR was done in all four (100%) patients, while CT chest was done in three (75%) patients (Table 3). The classical appearance of PJP on chest radiograph is bilateral perihilar or diffuse symmetrical interstitial pattern, which may be finely granular, reticular or ground-glass in appearance 13. The prominent CT findings are ground-glass opacity or consolidation with ill-defined centrilobular nodular air-space opacities ranging from 1 to 3 cm in size. *Hidalgo* et al. reported that GGO has 100% sensitivity, 86% specificity and 90% accuracy for diagnosing *Pneumocystis* pneumonia 20. Crazy paving appearance, mosaic attenuation pattern and cystic abnormalities may also be present. 21

In the present study, similar findings were observed on chest radiograph and CT scans of 2 patients with PJP infection (Figs. 16, 17). Out of these two patients of *PJP* infection, one patient improved with specific treatment for *PJP* infection, while other did not survive despite adequate management.

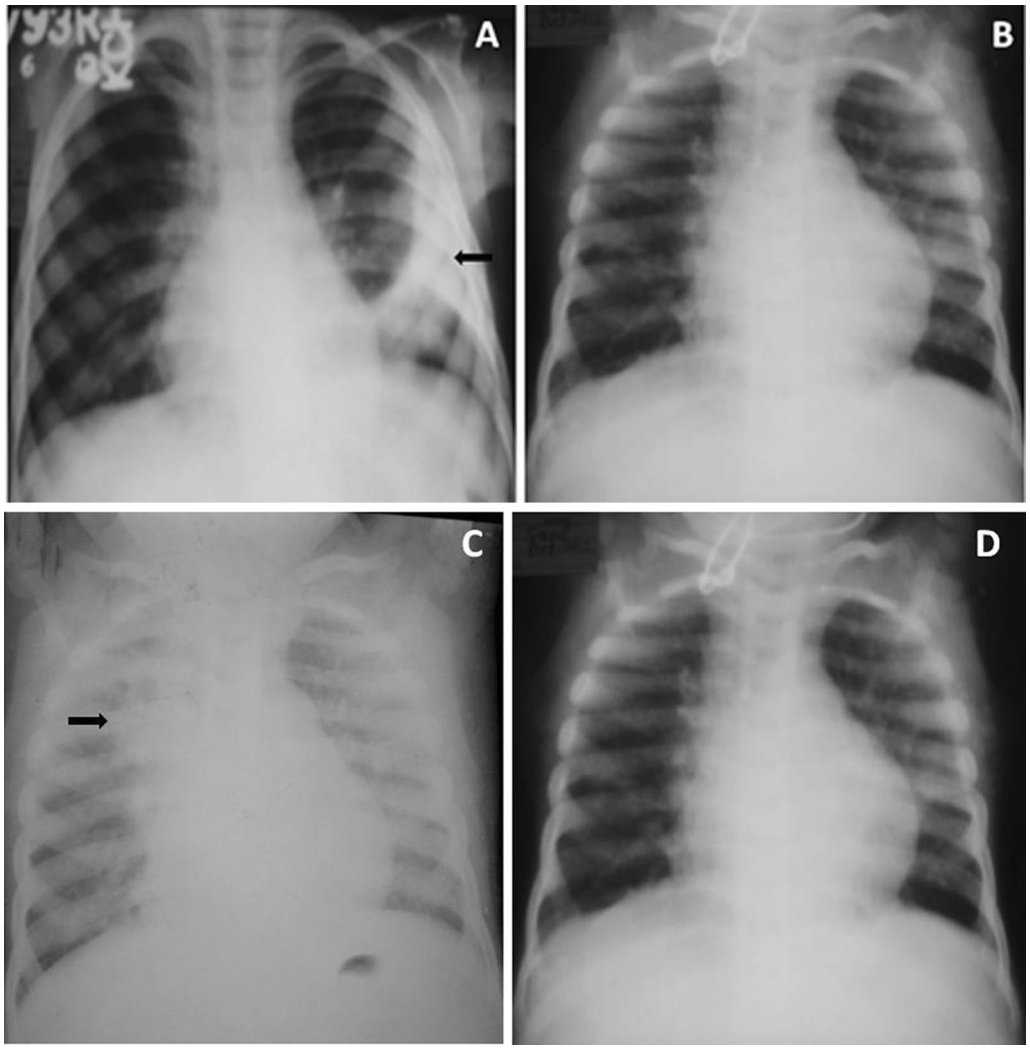

Fig. 14 Tubercular Infection (followed by polymicrobial infection). CXR in a 4-year-old female child, with complaints of chest pain, cough & low-grade fever for 2 weeks, shows left pleural effusion (arrow, **A**). Pleural tap was done and it revealed significantly raised LDH. However, no microorganism could be isolated. ATT was started and patient responded over a period of 4 months B). Later, she developed focal consolidation in right upper zone (arrow, **C**). CD4 count was 280 cells/$mm^{3.}$ BAL specimen isolated *Pseudomonas* and pneumococcus was isolated in sputum. She was given a course of antibiotics and her clinico-radiological profile improved (**D**) over a period of 4 weeks

Chest radiographic manifestation of pulmonary candidiasis includes patchy unilateral or bilateral air-space consolidation and poorly defined nodules 22. In our study, one patient with sputum positive candida infection revealed bilateral upper zone consolidation with ill-defined nodular opacities (1–3 cm size) in right lower zone (Fig. 18). The patient improved with specific antifungal treatment.

CXR versus CT chest in HIV-positive children

Our study showed that CT has higher sensitivity in all three types of infections as compared to CXR. However, CT is less helpful in patients with obvious radiographic abnormalities, leading to only a modest increase in diagnostic accuracy. CT is also of limited value in the detection and differential diagnosis in patients with more than one intrathoracic complications of AIDS. 23

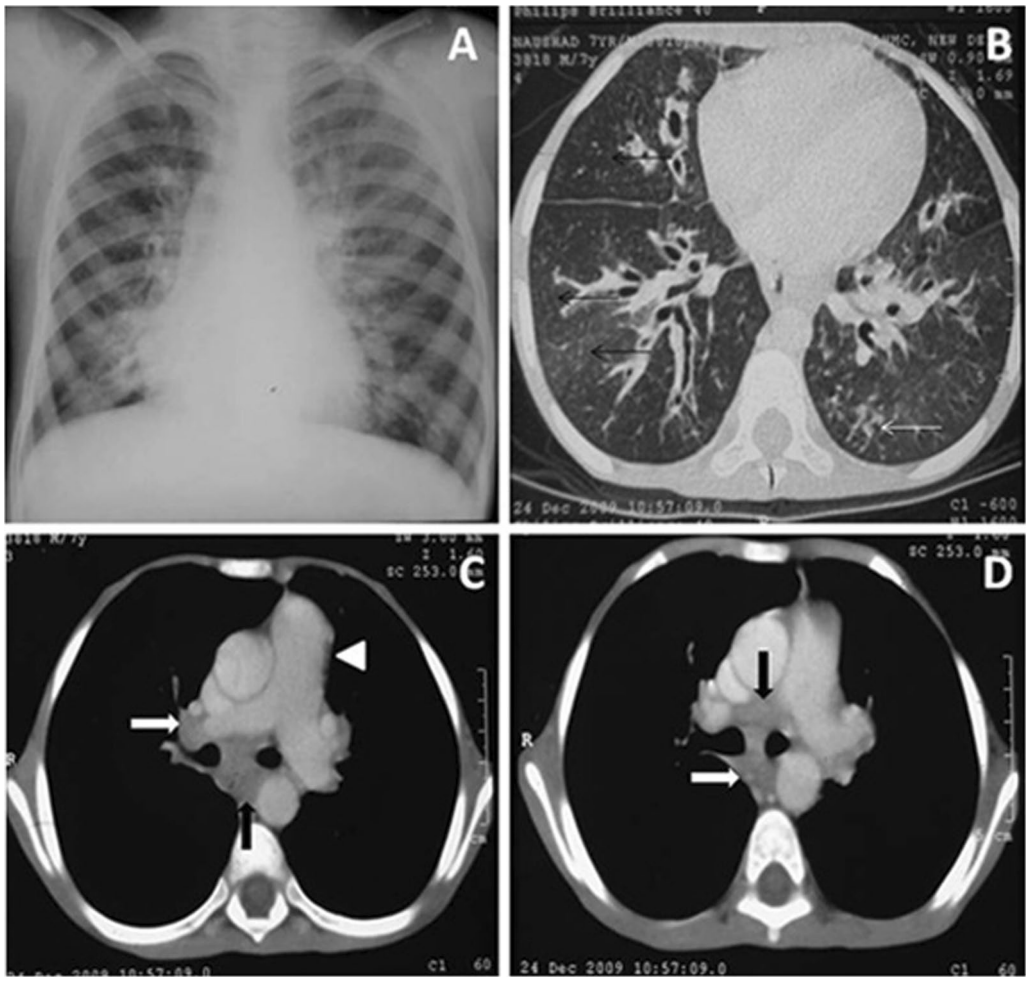

Fig. 15 Tubercular Infection. A 13-year-old HIV-positive male presented with cough and fever for 3 weeks. CXR (PA view) reveals right lower zone haze and bilateral central peribronchial thickening and bronchiectatic changes (**A**). Axial CECT chest (lung window) shows patchy areas of GGO involving bilateral lungs, centrilobular nodules in right lung (black arrows, B), and centrilobular nodules arranged in typical tree-in-bud appearance in left lower lobe (white arrow, **B**). Central cylindrical bronchiectasis with peribronchial thickening is also seen. The main pulmonary artery (arrowhead, **C**) is prominent as compared to ascending aorta suggesting pulmonary hypertension. Conglomerate mediastinal and hilar lymphadenopathy (with some of the nodes showing central necrosis) is also seen (arrows in **C**,**D**). CD4 count was 285 cells/cu.mm. BAL/sputum could not isolate any microorganism. ATT was started and the patient improved thereafter clinically

Limitations of the present study

The present study involved 45 HIV-positive children presenting in the institute. Such sample size may appear small while drawing broader conclusions, especially if geographic, economic and cultural considerations are taken into account. Multicenter studies with larger sample size may address this concern in future.

Conclusion

CXR is the initial imaging modality for assessment of pulmonary infections. It provides radiological base line before initiation of antiretroviral therapy and to monitor treatment response. CT is helpful in excluding or confirming the lung disease where CXR findings are normal or equivocal. Contemporary MDCT is a highly sensitive technique for delineation and characterization of parenchymal abnormalities and mediastinal lesions.

Combination of focal consolidation on chest radiograph and history of fever with productive cough

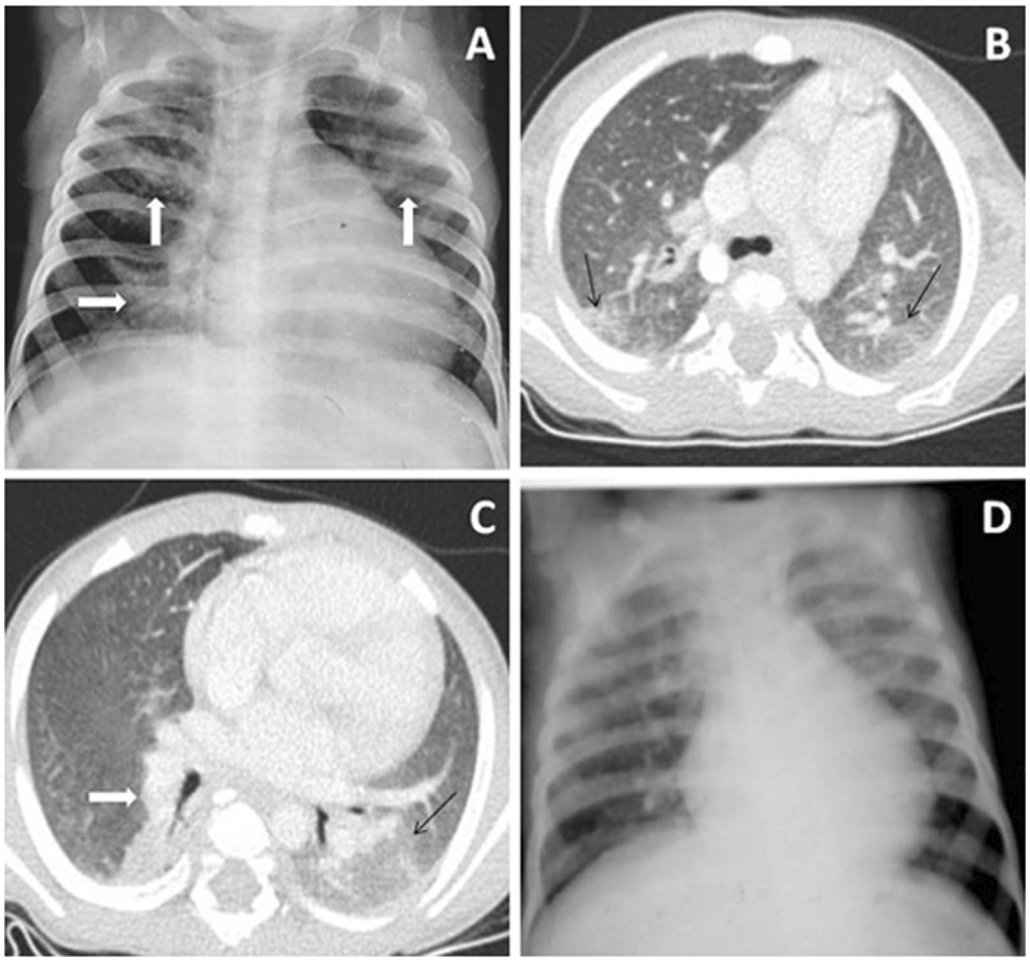

Fig. 16 Fungal Infection. Frontal CXR in an 18-month-old HIV-positive male child, presented with recurrent episodes of cough & fever for last 3 weeks, reveals inhomogeneous nodular opacities involving bilateral upper lung and right lower zone (arrows, **A**). CECT chest (axial, lung window) showed GGO in posterior part of bilateral upper lobes & posterior basal segment of LLL (black arrows in **B**,**C**), and dense consolidation involving apical, medial basal and posterior basal segments of RLL (white arrow, **C**). CD4 count was 172 cells/mm^3. Neutrophil count was 20%. BAL isolated *Pneumocystis jiroveci* and *Candida* species. Serial follow-up radiographs showed persistence of findings (**D**). Patient soon expired

for < 1 week duration has high sensitivity and specificity for the diagnosis of bacterial pneumonia. Symptoms for more than 3 weeks and central necrosis within enlarged hilar and/or mediastinal lymph nodes on CECT chest is highly suggestive of tubercular infection. GGO has high sensitivity and specificity for diagnosing fungal pneumonia, of which *Pneumocystis* is an important & common cause in HIV-positive children.

Bacterial pneumonias tend to occur throughout the course of HIV illness, becoming increasingly common with a falling CD4 count. Since they often occur at relatively high CD4 counts, bacterial infections tend to be the first pneumonic process to occur prior to the onset of full-blown AIIDS. Early in HIV infection, when CD4 count is > 200 cells/mm^3, the imaging features in pulmonary tuberculosis are typically those of post-primary tuberculosis, while in patients with decreased

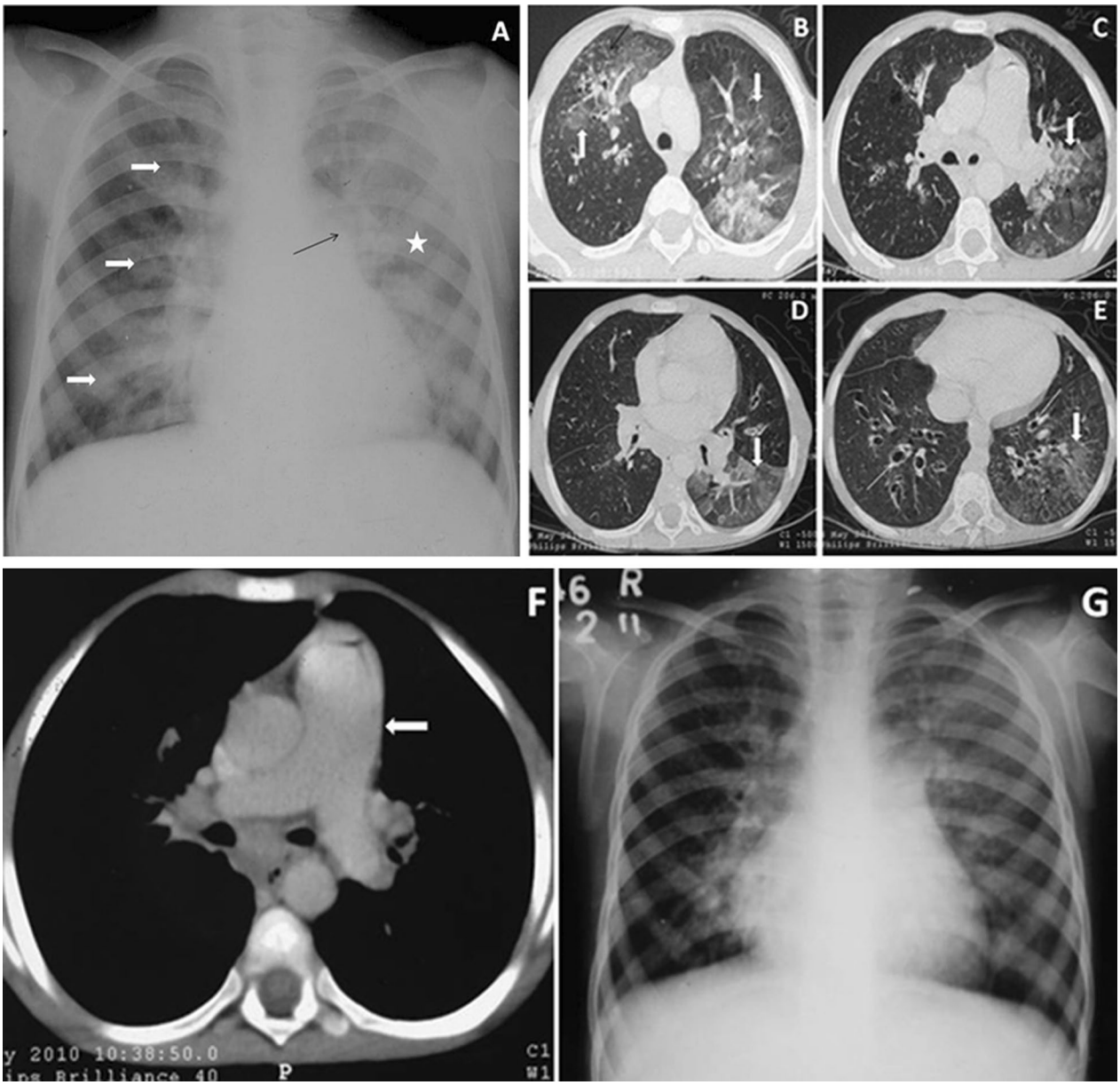

Fig. 17 Fungal Infection. Frontal chest radiograph in a 13-year-old HIV-positive male child, presented with fever & cough for 4 days, shows diffuse haze/GGO involving left lung (asterisk, **A**), and patchy areas of inhomogenous opacity in right lung (white arrows, **A**). Pulmonary bay fullness with peripheral pruning of pulmonary arteries (suggesting pulmonary hypertension) is evident (black arrow, **A**). CT scan (axial, lung window) shows GGO involving anterior segment of RUL, apico-posterior segment of LUL and superior, anteromedial & lateral basal segments of LLL (thick white arrows in B,C,D,E). Ill-defined centrilobular nodules are also visible in similar anatomic locations (black arrows in **B**,**C**). GGO along with interlobular septal thickening in superior segment of LLL gave crazy paving appearance to the involved segment (thick white arrow, **D**). Bilateral cystic & traction bronchiectatic changes are also present (thin white arrows, **E**). Enlarged pulmonary artery suggestive of pulmonary hypertension (arrow, **F**) is evident on axial CECT chest (mediastinal window). CD4 count was 131 cells/cu.mm. BAL/sputum did not isolate any microorganism. Patient was clinically sick and hypoxic. On the basis of clinical and radiological findings, a probable diagnosis of *Pneumocystis jiroveci* pneumonia was made. Patient was treated with trimethoprim/sulfamethoxazole combination and improved clinically as well as radiologically (**G**)

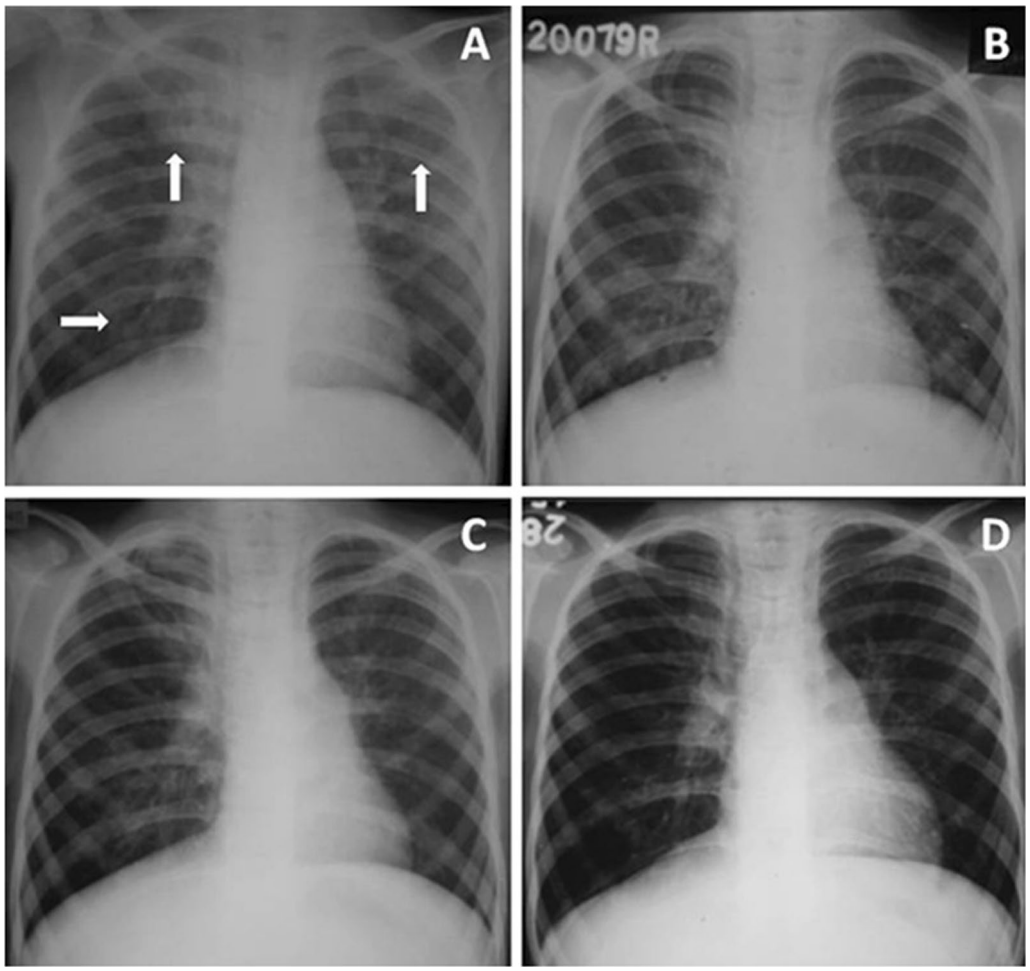

Fig. 18 Fungal Infection. A 12-year-old HIV-positive male, presented with fever and cough of 1 week duration. CXR (PA view) reveals inhomogeneous opacity involving bilateral upper zones and right lower zone (arrows, **A**). Patient showed no improvement after antibacterial treatment for 3 weeks. Sputum sample isolated *Candida* species. CD4 count was 147 cells/cu.mm. Neutrophil count was 35%. Patient was put on antifungal treatment, serial chest radiographs (**B**,**C**,**D**) showed gradual resolution of opacities over a period of 4–5 months

cell counts of < 200 cells/mm^3, findings are more typically those of primary tuberculosis. Patients with fungal infection are severely immunocompromised, almost always having CD4 counts < 200 cells/mm^3.

Acknowledgements
Not applicable.

Author contributions
All the authors have significantly contributed in the study.

Funding
None.

Availability of data and materials
The datasets generated and/or analyzed during the current study are not publicly available due to data being hospital patients' details, but are available from the corresponding author on reasonable request.

Declarations

Ethics approval and consent to participate
Yes, obtained from Institutional Ethical Committee, Lady Hardinge Medical College, New Delhi, India.

Consent for publication
Yes.

Competing interests
The author declares that there is no competing interest.

Author details
[1]Department of Radiology, Burjeel Royal Hospital, Abu Dhabi, UAE. [2]Department of Radiodiagnosis, Lady Hardinge Medical College, New Delhi 110001, India. [3]Department of Radiodiagnosis, Atal Bihari Vajpayee Institute of Medical Sciences and Dr. Ram Manohar Lohia Hospital, New Delhi 110001, India. [4]Department of Pediatrics, Lady Hardinge Medical College, New Delhi 110001, India. [5]Department of Microbiology, Maulana Azad Medical College, New Delhi 110001, India.

Received: 25 September 2023 Accepted: 20 March 2024
Published online: 04 April 2024

References

1. World Health Organization. HIV data and statistics. WHO. Available from: https://www.who.int/teams/global-hiv-hepatitis-and-stis-programmes/hiv/strategic-information/hiv-data-and-statistics. Accessed January 10, 2024
2. World Health Organization. Treatment and care in children and adolescents. WHO. Available from: https://www.who.int/teams/global-hiv-hepatitis-and-stis-programmes/hiv/treatment/treatment-and-care-in-children-and-adolescents. Accessed January 10, 2024.
3. Marks MJ, Haney PJ, McDermott MP, White CS, Vennos AD (1996) Thoracic diseases in children with AIDS. Radiographics 16:1349–1362
4. Plessis VD, Andronikou S, Struck G, McKerrow N, Stoker A (2011) Baseline chest radiographic features of HIV-infected children eligible for antiretroviral therapy. South Africa Med J 101:829–834
5. Gona P, Van Dyke RB, Williams PL, Dankner WM, Chernoff MC, Nachman SA et al (2006) Incidence of opportunistic and other infections in HIV-infected children in the HAART era. JAMA 296:292–300
6. Shah R, Kaji A, Ostrum B, Friedmann A (1997) Interpretation of chest radiographs in AIDS patients: usefulness of CD4 lymphocyte counts. Radiographics 17:47–58
7. avert.org [Internet]. UK: HIV and AIDS in India; c2017 [updated 2018 Oct 26; cited 2018 Nov 10]. Available from: https://www.avert.org/professionals/hiv-around-world/asia-pacific/india
8. Afeseen B, Green W (2000) Bacterial pneumonia in hospitalized patients with HIV infection. Chest 117:1017–1022
9. Hirschtick RE, Glassroth J, Jordan MC (1995) Bacterial pneumonia in persons infected with human immunodeficiency virus. N Eng J Med 333:845–851
10. Sider L, Gabriel H, Curry DR, Pham MS (1993) Pattern recognition of the pulmonary manifestations of AIDS on CT scans. Radiographics 13:771–784
11. Jasmer RM, Edinburgh KJ, Thompson A (2000) Clinical and radiographic predictors of pulmonary nodules in HIV-infected patients. Chest 117:1023–1030
12. Aviram G, Fishman JE, Sagar M (2001) Cavitary lung disease in AIDS: etiologies and correlation with immune status. AIDS Patient Care STDS 15:353–356
13. Boiselle PM, Tocino I, Hooley RJ (1997) Chest radiograph diagnosis of pneumocystis carinii pneumonia, bacterial pneumonia and pulmonary tuberculosis in HIV-positive patients: accuracy, distinguishing features and mimics. J thoracic Imaging 12:47–53
14. Madhivanan P, Mothi SN, Kuarswamy N, Yepthomi T, Venkatesan C, Lambert JS et al (2003) Clinical manifestations of HIV-infected children. Indian Journal Pediatr 70:615–620
15. Pol RR, Shepur TA, Ratageri VH (2007) Clinico-laboratory profile of pediatric HIV in Karnataka. Indian J Pediatr 74:1071–1075
16. Hesseling AC, Westra AE, Werschkull H, Donald PR, Beyers N, Hussey GD et al (2005) Outcome of HIV-infected children with culture confirmed tuberculosis. Arc Dis Child 90:1171–1174
17. Saurborn DP, Fishman JE, Boiselle PM (2002) The imaging spectrum of pulmonary tuberculosis in AIDS. J thorac Imaging 17:28–33
18. Lenug AN (1999) Pulmonary tuberculosis: the essentials. Radiology 210:307–322
19. Laissey JP, Cadi M, Boudiaf ZE (1998) Pulmonary tuberculosis: Computed tomography and high resolution computed tomography patterns in patients who are either HIV-negative or HIV-seropositive. J Thoracic Imaging 13:58–64
20. Morris A, Lundgren JD, Masur H (2004) Current epidemiology of pneumocystis pneumonia. Emerg Infect Dis 10:1713–1720
21. Hidalgo A, Falco V, Mauleon S, Andreu J, Crespo M, Ribera E (2003) Accuracy of high resolution CT in distinguishing between Pneumocystis carinii pneumonia and non-pneumocystis carinii pneumonia in AIDS patients. Eur Radiol 13:1179–1184
22. Buff SJ, McLelland R, Gallis HA (1982) Candida albicans pneumonia: radiographic appearance. AJR Am J Roentgenol 138:645–648
23. Kang EY, Staples CA, Mc Guinness G, Primack SL, Muller NL (1996) Detection and differential diagnosis of pulmonary infections and tumors in patients with AIDS: value of chest radiography versus CT. AJR Am J Roentgenol 166:15–19

Publisher's Note